https://doi.org/10.48048/tis.2023.5169

Anomalous Variations in Ionosphere TEC Before the Earthquakes of 2021 in the Different Parts of the Globe

Kunvar Shardaprasad Yadav, Rakesh Bhikhabhai Vadnathani*, Keyurgiri Rajendragiri Goswami and Priyanka Mahesh Patel

Department of Physics, Faculty of Science, Mehsana Urban Institute of Science, Ganpat University, Gujarat 384012, India

(*Corresponding author's e-mail: vadnathanirakesh165@gmail.com)

Received: 11 July 2022, Revised: 30 August 2022, Accepted: 6 September 2022, Published: 25 April 2023

Abstract

The present article shows the satellite-based TEC data analysis for 6 earthquakes ($M \geq 6.0$) from specific parts of the earth that occurred in 2021 during the low solar radiation period. In search of pre-earthquake signatures in the ionosphere, the study of the data of GPS-based TEC before the earthquake is needed. L_1 and L_2 frequency delays have shown STEC and VTEC formulations for Ionosphere electron density measurements. The TEC data shows unusual behavior from 1 to 30 days before an earthquake. The primary goal of this article is to investigate and establish the correlation of lithosphere atmosphere coupling before earthquakes. Dst and $F_{10.7}$ solar flux parameters have shown solar radiation. Additionally, TEC data also represented as heat maps to confirm their location at the epicenter. This research might help us understand how ionosphere properties respond to seismic activity in the earth's crust.

Keywords: Total electron content (Tec), Earthquake, Slant total electron content (STEC), Vertical total electron content (VTEC), Disturbance storm time index (Dst), $F_{10.7}$ (solar flux), Global positioning system (GPS), International GNSS service (GNSS), Receiver independent exchange format (RINEX)

Introduction

We are all aware that earthquakes are a frequent, naturally occurring phenomenon all over the Globe. The earth's core and some surrounding layers interactive mechanism are essential to understand earthquake preparation. Science underlies the movement of plates that causes an earthquake; the earth's structure is composed of several plates, including some minor plates and 7 significant plates. The heat that accumulates in the core causes these plates to be continually in circulation, gliding, clashing and drifting apart [1]. We are aware that earthquakes of a larger magnitude cause significant economic harm and claim a larger number of lives; they also change the region's topography around its epicentre. Changes in the earth's lower atmosphere, like changing the troposphere's temperature because of IR (infrared) emission, the vertical profile of humidity, and pressure [2]. Variations in the upper atmosphere occurred due to anomalies in parameters such as ionization, quasi-stationary electric fields [3], and ionospheric parameter TEC. (TEC is Total Electron Content, Also known as electron density in 1 m^2. Which is 1 TCEU = 1×10^{16} electron/m^2 were recorded above the seismic regions. The troposphere is the closest layer to the earth's surface; therefore, it is the densest layer. Earthquakes cause immediate changes to the troposphere. These changes are because of the release of gases (radon gas emission) from deep inside the earth. Leakage of this radon gas from the earth's surface because of the earthquakes are the reason for temperature rising and humidity changes in the surrounding area [4]. Because of a more significant concentration of electrons, the ionosphere is a worldwide electric current, which is TEC (Total Electron Content, density of electrons in ionosphere). Many natural events, such as dust storms, thunderstorms [5], earthquakes, volcanic activity [6], radioactive gases [7], and solar radiation [8], induce variations in density of TEC. TEC rose during the previous high solar radiation cycle, which occurred in 2014 - 2015; during this time, high-energy solar particles made contact with the earth's ionosphere, causing TEC to shift.

Data

Earthquake data

The site used to collect data was (https://earthquake.usgs.gov). **Table 1** shows a list of earthquakes for the study of seismo-ionospheric correlation.

Table 1 Data of 6 earthquakes that occurred in 2021.

Sr. No.	Location of epicenter (latitude, longitude) Magnitude	Date	Time (UT)	IGS stations and their locations
1	Kermadec Islands, New Zealand (29°43′S, 177°17′W) M 8.1	04/03/2021	19:28	WARK (New Zealand) (36°26′S, 174°40′E)
2	Gisborne, New Zealand (37°29′S, 179°27′E) M 7.3	04/03/2021	13:27	WGTN (New Zealand) (41°19′S, 174°48′E)
3	Chickaloon, Alaska (62°26′N, 148°15′W) M 6.1	31/05/2021	06:59	FAIR (Alaska, USA) (64°59′N, 147°30′W)
4	Pocito, Argentina (31°50′S, 68°48′W) M 6.4	19/01/2021	02:46	SANT (Chile) (33°9′S, 70°40′W)
5	Japan (38°12′N, 141°36′E) M 6.9	01/05/2021	07:33	SMST (Japan) (33°35′N, 135°56′E)
6	Ishinomaki, Japan (38°27′N, 141°38′E) M 7.0	20/03/2021	09:09	USUD (Japan) (36°8′N, 138°22′E)

TEC data

The P_1 (c/a code pseudo-range) in meters, P_2 (p-code pseudo-range, in meters, L_1 (L_1 carrier phase) on f_1 frequency), and L_2 (L_2 carrier phase on f_2 frequency) with a time resolution of 30 s are all included in the RINEX data obtained from GPS receivers. From an IGS data collection in RINEX format, the STEC (slant total electron content) was calculated by;

$$STEC = \left(\frac{f_1^2 f_2^2}{f_1^2 - f_2^2}\right)\left(\frac{P_1 - P_2}{40.3}\right) \quad (1)$$

The current GPS broadcast frequencies are f_1 (1,227.60 MHz) and f_2(1,575.42 MHz).

Using an appropriate mapping function of distinct ionosphere pierce point (IPP) location, STEC transformed to VTEC, and the mapping function S(E) was defined as follows;

$$S(E) = \frac{1}{\cos \chi'} \quad (2)$$

$$VTEC = \frac{STEC}{S(E)} \quad (3)$$

where,

$$\cos \chi' = \sqrt{1 - \left(\frac{R_x \cos \chi^2}{R_x + h_m}\right)} \quad (4)$$

R_x = Earth mean radius, 6,371 km, χ = angle of elevation, χ' is zenith angle, and h_m = 350 km (IPP), is the ionospheric shell's height above the earth's surface [9]. We compute the median X of the 30 days before and after the earthquake date and the VTEC value in the Y median in this study to discover an abnormality in ionospheric TEC.

Analysis

A GPS RINEX algorithm developed by Dr. Gopi Krishna Seemala, Indian Institute of Geomagnetism (IIG), Navi Mumbai, India, was used to extract text files of tec from the CDDS website from the satellite. The process yielded CMN files for each earthquake. With the help of Lab-VIEW codes, VTEC data have been obtained every hour for 60 days.

Results

Various data of earthquakes showed VTEC peaks, Dst-index, and solar flux. It has shown in **Table 1** the data of 6 different earthquakes; the below graphs show variations in TEC of the ionosphere because of those earthquakes. The first graphs of each earthquake show data of TEC v/s date, which shows no correlation between latitude and longitude of the earthquake's coordinates and the tec variations. The second graph of each earthquake fulfills this condition of low solar activity.

Earthquake of New Zealand (M 8.1)

An earthquake on March 04 (marked by a green star) shook the Kermadec island region in New Zealand; an anomaly in TEC have observed on February 06, February 21, February 28, March 06, March 14 and March 25, as shown in **Figure 1(a)**. The solar activity is not observed on the Day, as shown in **Figure 1(b)**.

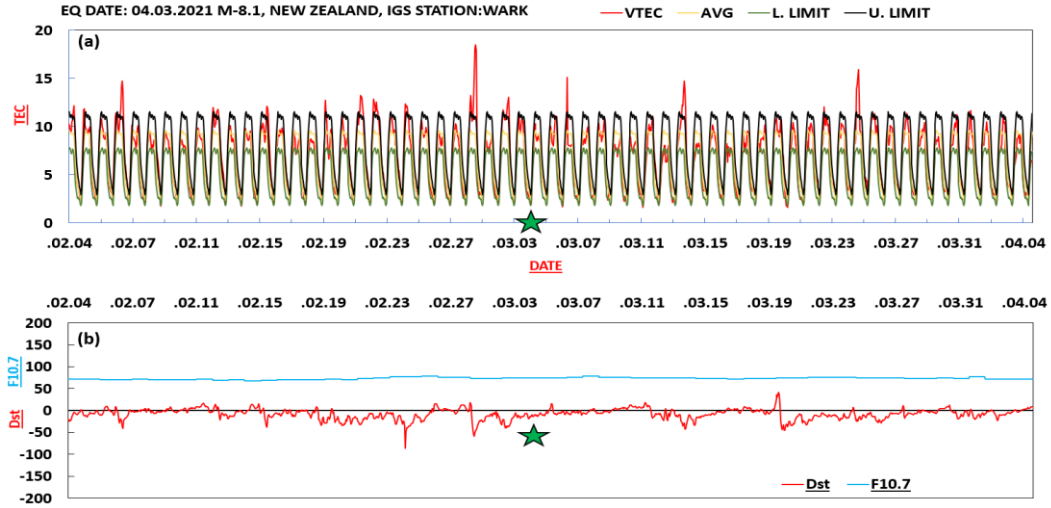

Figure 1 (a) VTEC profile of the Kermadec Island, New Zealand (WARK) station; the daily VTEC curve shows an increase in diurnal VTEC (red line). Before the earthquake, the black line shows 75 % of the max VTEC value for 60 days; if any peak goes above black VTEC, it is considered an anomalous variation of tec (yellow and green lines show the average value of VTEC and the lower limit of VTEC accordingly). (b) The figure displays solar flux $F_{10.7}$ on top with a blue line and Dst-index with a red line. The geomagnetic situation is considered tranquil, with a modest fluctuation in the Dst-index. The star symbol represents the day of the earthquake.

The coordinates of the Kermadec island, New Zealand earthquake of 8.1 M, are −29.7228 (latitude) and −177.2794 (longitude). The anomalous effect of earthquakes is in the range of 500 - 600 km from the earthquake's epicenter since the earthquake's magnitude is very high. **Figure 2** (heat map form) shows the latitude data v/s Day while VTEC has shown on the z-axis. Similar results have been reported by [10].

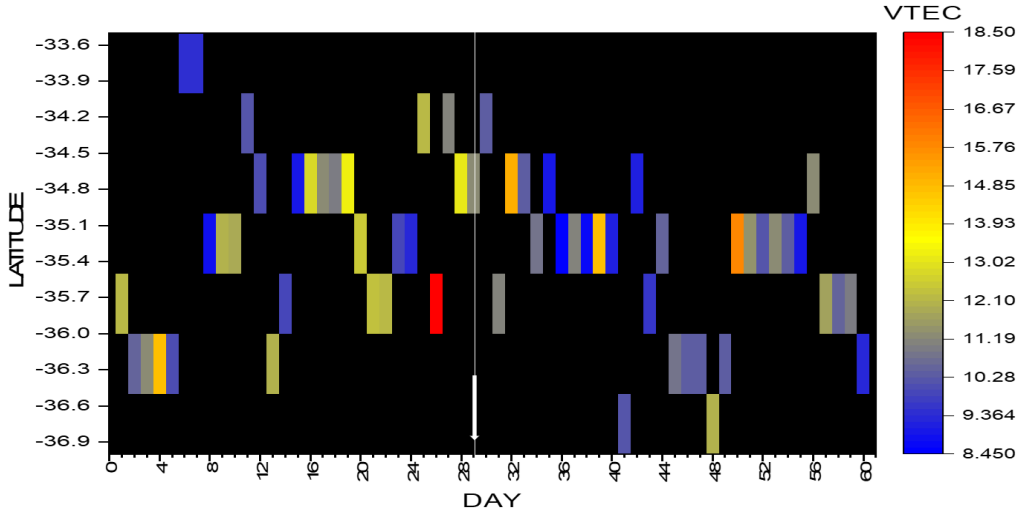

Figure 2 The heat map representation of VTEC in latitude v/s Day. This data shows the increment in TEC for 60 days. The plot values greater than 11.45833×10^{16} TECU (total electron content unit) can be considered anomalous VTEC. The yellow and red lines are in the regions close to the earthquake's epicenter. The white arrow indicates the Day of the earthquake.

Earthquake of New Zealand (M 7.3)

This graph shows an earthquake that occurred in New Zealand on March 04, 2021, but this data is from a different satellite named WGTN. TEC variations are above the standard deviation line on February 03, February 07, February 16, March 01, March 13 and 25th march **Figure 3(a)**. Which are almost similar to the data we collected from satellite WARK. No solar radiation exists in this period; $F_{10.7}$ is silent during this high TEC period. **Figure 3(b)**. The earthquake was on March 04.

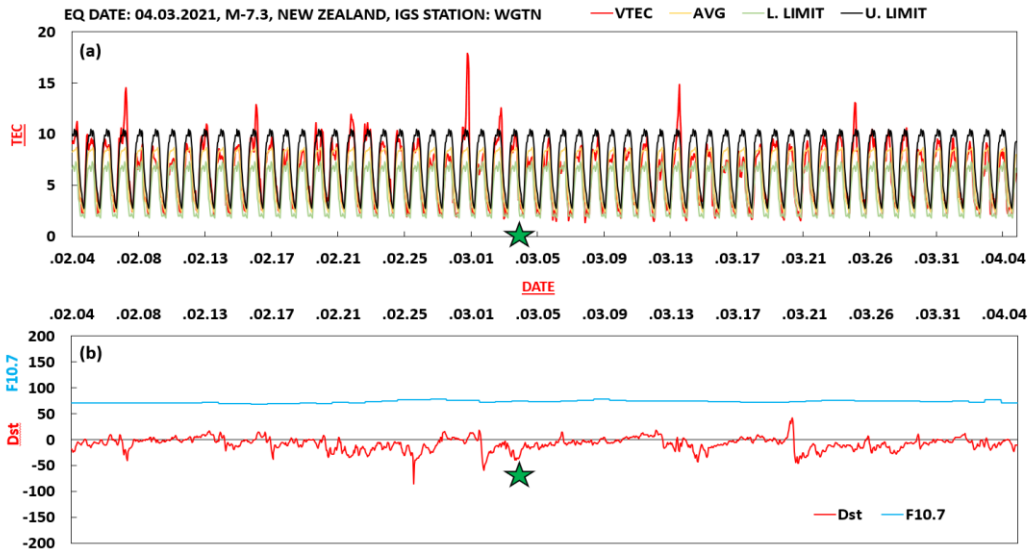

Figure 3 (a) VTEC profile of the Kermadec Island, New Zealand (WGTN) station; the daily VTEC curve shows an increase in diurnal VTEC (red line) before the earthquake. TEC anomalies on 3/2, 7/2, 16/2, 1/3, 13/3 and 25/3. (b) Displays solar flux $F_{10.7}$ on top with the blue line and Dst-index with a red line. The geomagnetic situation is considered tranquil, with a modest fluctuation in the Dst-index. The star symbol represents the day of the earthquake.

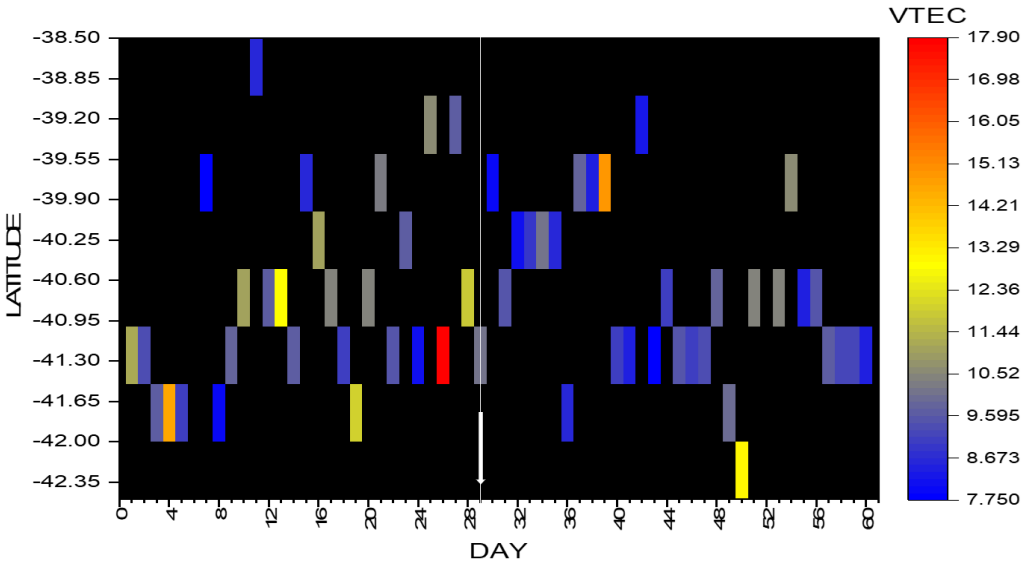

Figure 4 The heat map representation of VTEC in Latitude v/s Day. This data shows the maximum VTEC of each day for all 60 days. Higher than 10.52222×10^{16} TECU (Total electron content unit) indicates an anomaly in VTEC as we can see that most of the yellow and red lines are in the regions close to the epicenter of the earthquake. The white arrow shows the day of the earthquake.

Earthquake of Alaska (M 6.1)

This graph shows data of an earthquake that shook Alaska on May 31, 2021; data from TEC is from satellite FAIR. As we can see, TEC peaks are on May 17 and May 27 on and above the standard deviation line, which is not normal **Figure 5(a)** and not because of the solar flux $F_{10.7}$ **Figure 5(b)** since their values are not as high as it is required to cause such high variations in TEC. The earthquake is on May 31.

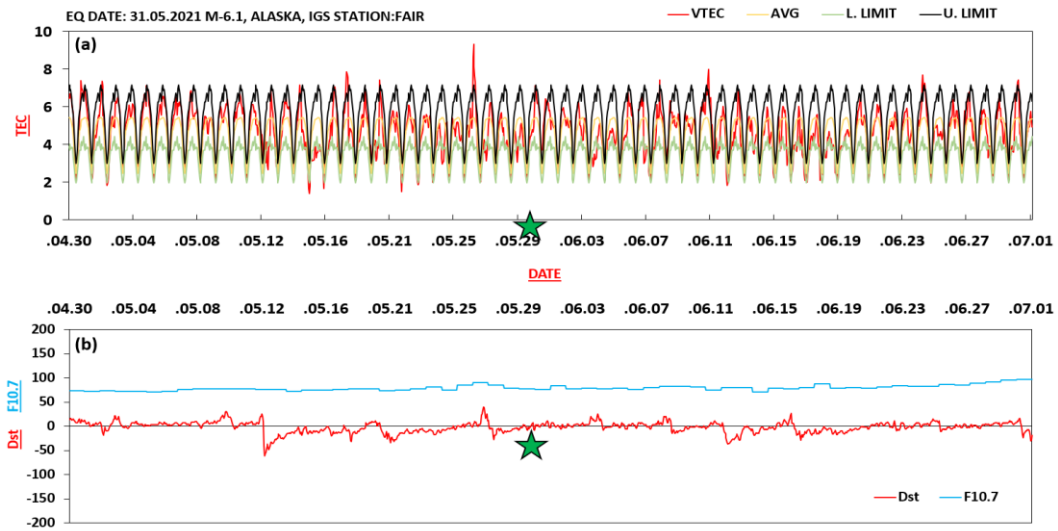

Figure 5 (a) VTEC profile of the Chickaloon, Alaska (FAIR) station; the daily VTEC curve shows an increase in diurnal VTEC (red line) before the earthquake; anomalous variations in TEC are on 17/5, 27/5, 11/6 and 25/6. (b) The figure displays solar flux $F_{10.7}$ on top with the blue line and Dst-index with the red line. The geomagnetic situation is considered tranquil, with a modest fluctuation in the Dst-index. The star symbol represents the day of the earthquake.

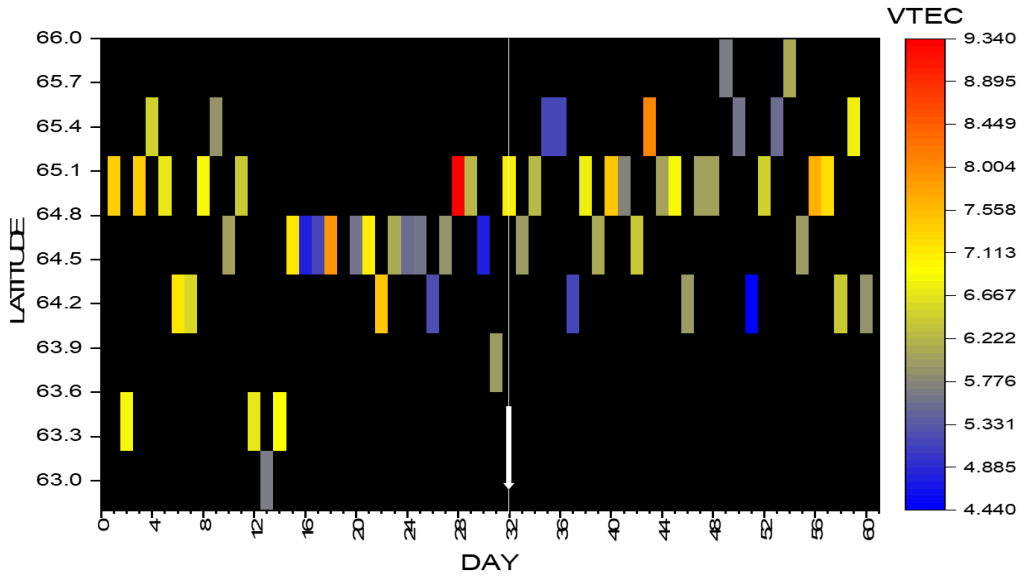

Figure 6 The heat map representation of VTEC in Latitude v/s Day. This data shows the maximum VTEC of each day for all 60 days. TEC greater than 7.17778×10^{16} TECU (Total electron content unit) indicates an anomaly in VTEC as we can see that most of the yellow and red lines are in the regions close to the epicenter of the earthquake. The white arrow shows the day of the earthquake.

Earthquake of Argentina (M 6.4)

The plot shows TEC data of an earthquake in Argentina on January 19, 202. It can be observed in **Figure 7(a)** January 02, January 03, and January 04. **Figure 7(b)** indicate an entirely solar day from plot Dst and $F_{10.7}$.

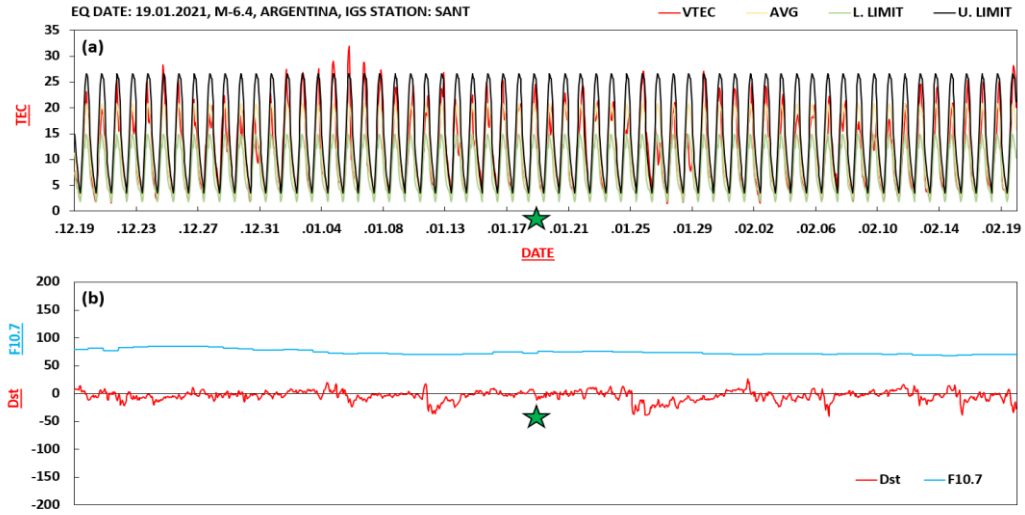

Figure 7 (a) VTEC profile of the Pacito, Argentina (SANT) station; the daily VTEC curve shows an increase in diurnal VTEC (Red line) before the earthquake; Anomalous Variations in TEC are on 2/1, 3/1, and 4/1 continuously. (b) The figure displays solar flux $F_{10.7}$ on top with the blue line and Dst-index with the red line. The geomagnetic situation is considered tranquil, with a modest fluctuation in the Dst-index. The star symbol represents the day of the earthquake.

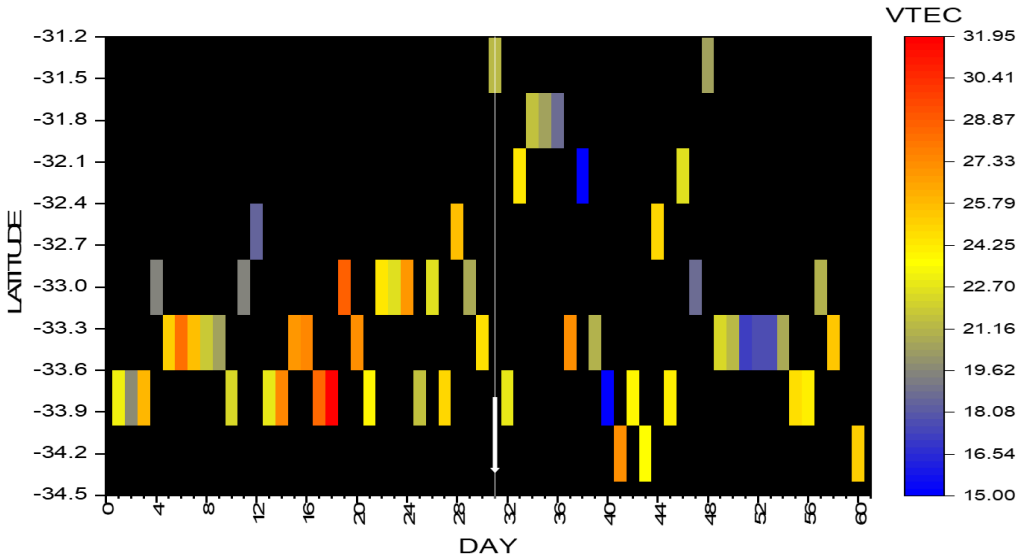

Figure 8 The heat map representation of VTEC in Latitude v/s Day. This data shows the maximum VTEC of each day for all 60 days. Higher than 26.06167×10^{16} TECU (Total electron content unit) indicates an anomaly in VTEC, as we can see that most of the yellow and red lines are in the regions close to the epicenter of the earthquake. The white arrow shows the day of the earthquake.

Earthquake of Japan (M 6.9)

Figure 9 shows an earthquake from Japan on May 01, 2021. There are 2 peaks in TEC right before the earthquake on April 25 and April 27, which are above the deviation line drawn out above 20 TECU (Total Electron Content Unit) **Figures 9(a) - 9(b)** shows data of $F_{10.7}$ and Dst.

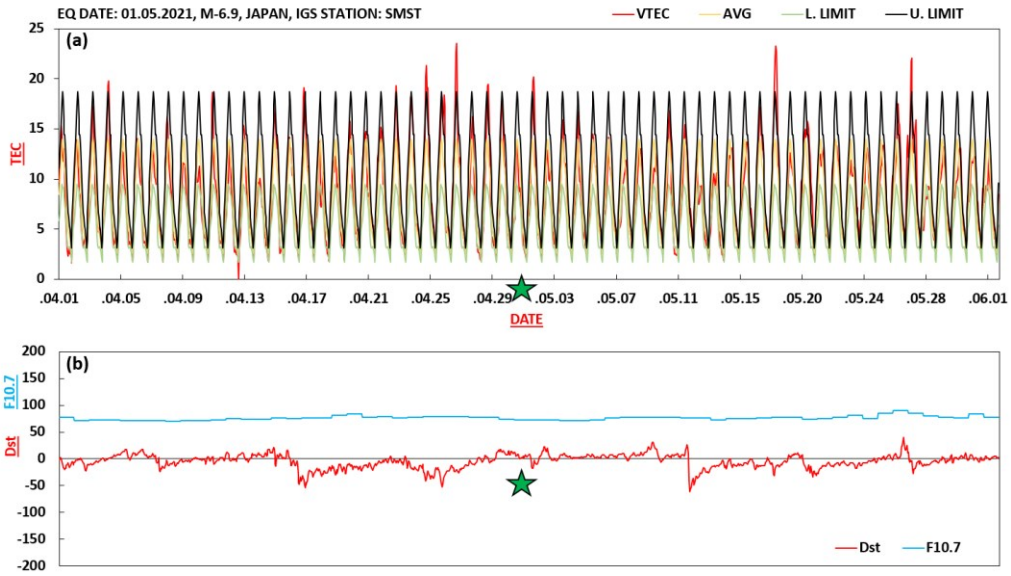

Figure 9 (a) VTEC profile of the Japan (SMST) station; the daily VTEC curve shows an increase in diurnal VTEC (Red line) prior to the earthquake; Anomalous Variations in TEC are on 25/4, 27/4, 2/5, 18/5 and 27/5. (b) The figure displays solar flux $F_{10.7}$ on top with the blue line and Dst-index with the red line. The geomagnetic situation is considered tranquil, with a modest fluctuation in the Dst-index. The star symbol represents the day of the earthquake.

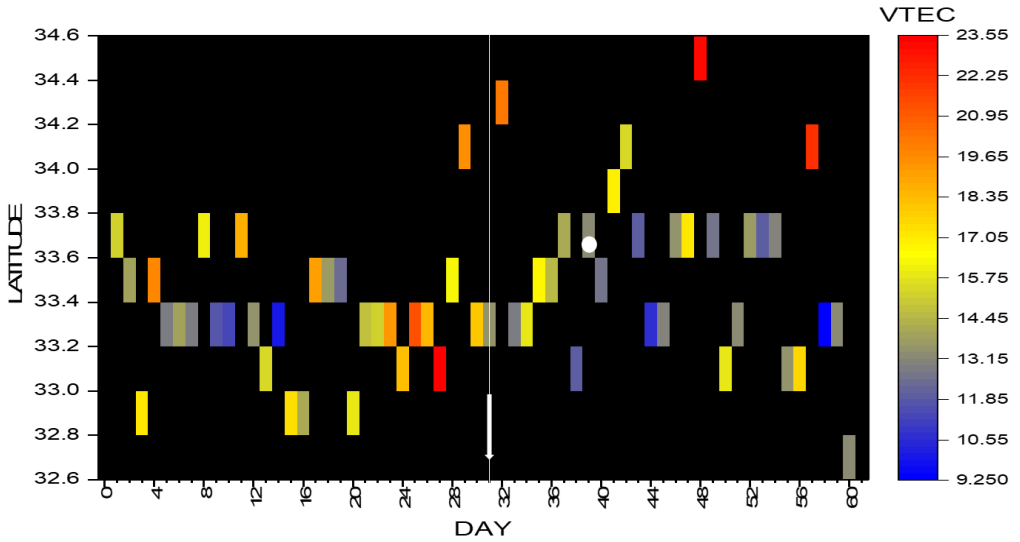

Figure 10 The heat map representation of VTEC in Latitude v/s Day. This data shows the maximum VTEC of each day for all 60 days. Higher than 18.66111×10^{16} TECU (Total electron content unit) indicates an anomaly in VTEC, as we can see that most of the yellow and red lines are in the regions close to the epicenter of the earthquake. The white arrow shows the day of the earthquake.

Earthquake of Japan (M 7.0)

This graph shows data of an earthquake that occurred in Japan on March 20, 2021; data from TEC is from satellite USUD. Anomalous behavior of TEC on February 19, February 22, February 28, March 02, March 05 and March 13 above the standard deviation line.

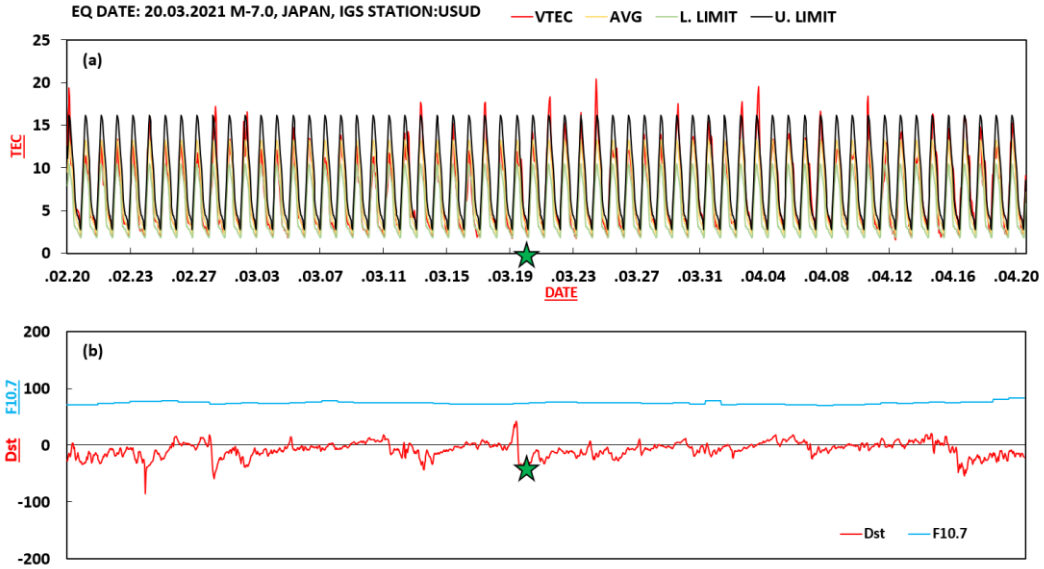

Figure 11 (a) VTEC profile of the Japan (USUD) station; the daily VTEC curve shows an increase in diurnal VTEC (Red line) prior to the earthquake; anomalous variations in TEC are on 19/2, 22/2, 28/2, 2/3, 5/3 and 13/3. (b) The figure displays solar flux $F_{10.7}$ on top with the blue line and Dst-index with the red line. The geomagnetic situation is considered tranquil, with a modest fluctuation in the Dst-index. The star symbol represents the Day of the earthquake.

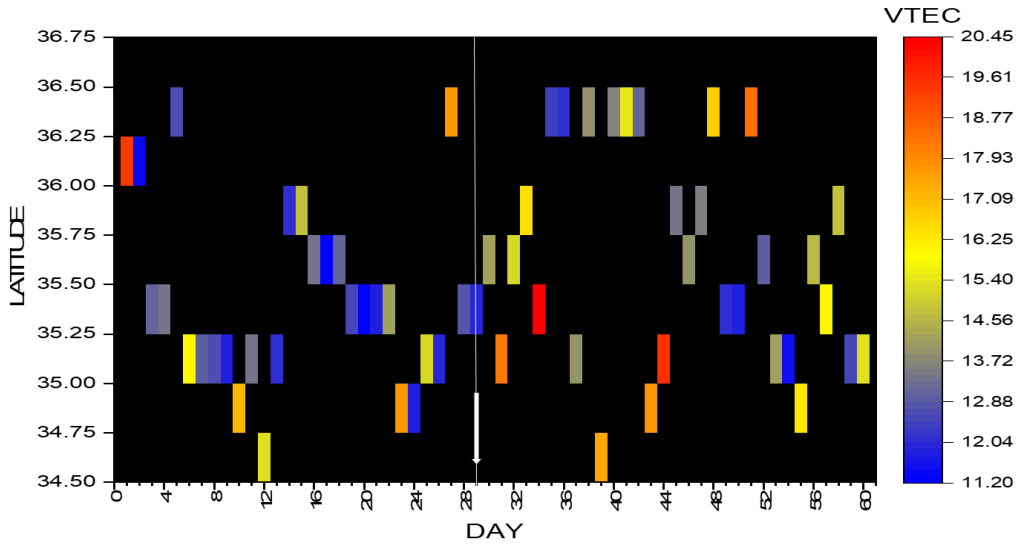

Figure 12 The heat map representation of VTEC in Latitude v/s Day. This data shows the maximum VTEC of each day for all 60 days. Higher than 16.16096×10^{16} TECU (Total electron content unit) indicates an anomaly in VTEC, as we can see that most of the yellow and red lines are in the regions close to the epicenter of the earthquake. The white arrow shows the Day of the earthquake.

The purpose of study from further down is to indicate TEC variations of a particular region throughout the year. These results serve as a way to show seasonal variations of TEC over a New Zealand region, which is useful for separating out anomalous VTEC for seismic activity. In New Zealand, the summer season lasts from December to March and the winter season lasts from June to August. The temperature ranges between winter and summer in the rest of the year. Stars shows the Earthquakes occurred in the WARK igs station region. **Table 2** shows the data of earthquake $M \geq 6$ occurred in New Zealand 2021.

Table 2 Earthquakes occurred in the working region of WARK00NZL igs station over the year of 2021.

Sr. No.	Location of earthquakes (coordinates), Magnitude	Date	Days with TEC anomalies prior to 30 days of Earthquake day
1	Kermadec Island, New Zealand (29.4295S, 178.744W) M 6.3	08/01/2021	01/01, 02/01, 06/01
2	Loyalty Islands (23.0511S, 171.657E) M 7.7	10/02/2021	19/01, 26/01, 02/02, 04/02, 07/02
3	Loyalty Islands (23.1842S, 171.779E), M 6.1	17/02/2021	26/01, 02/02, 04/02, 07/02
4	Gisborne, New Zealand (37.4787S, 179.481E), M 7.3	04/03/2021	01/03, 03/03
	Kermadec Island, New Zealand (29.7228S, 177.279W), M 8.1	04/03/2021	01/03, 03/03
5	Kermadec Island, New Zealand (28.749S, 176.558W), M 6.3	05/03/2021	01/03, 03/03
6	Gisborne, New Zealand (37.5763S, 179.5947E), M 6.3	06/03/2021	01/03, 03/03
7	Kermadec Island, New Zealand (29.961S, 177.676W), M 6.4	01/04/2021	14/03, 23/03, 25/03, 26/03, 28/03
8	Gisborne, New Zealand (37.46S, 179.6324E), M 6.1	05/04/2021	14/03, 23/03, 25/03, 26/03, 28/03

Sr. No.	Location of earthquakes (coordinates), Magnitude	Date	Days with TEC anomalies prior to 30 days of Earthquake day
9	Kermadec Island, New Zealand (29.0489S, 176.6124W), M 6.1	07/04/2021	14/03, 23/03, 25/03, 26/03, 28/03
10	Pangai, Tonga (18.9036S, 176.27W), M 6.5	24/04/2021	25/03, 26/03, 28/03, 17/04, 18/04, 24/04
11	Haveluloto, Tonga (21.6097S, 177.153W), M 6.5	25/04/2021	25/03, 26/03, 28/03, 17/04, 18/04, 24/04
12	Kermadec Island, New Zealand (29.339S, 176.321W), M 6.1	29/04/2021	17/04, 18/04, 24/04
13	Kermadec Island, New Zealand (30.2162S, 177.845W), M 6.5	20/06/2021	06/06, 07/06, 08/06, 11/06, 12/06, 13/06, 16/06, 17/06, 18/06
14	Fiji (21.8116S, 179.864W), M 6.1	02/07/2021	11/06, 12/06, 13/06, 16/06, 17/06, 18/06, 25/06, 26/06, 27/06, 28/06, 30/06, 01/07
15	Kermadec Island, New Zealand (29.9271S, 176.864W), M 6.1	24/07/2021	01/07, 03/07, 08/07, 21/07, 22/07, 23/07, 24/07, 25/07
16	Kermadec Island, New Zealand (29.9211S, 177.38W), M 6.4	31/08/2021	03/08, 20/08, 21/08, 25/08, 26/08, 27/08, 28/08, 30/08
17	Vanuatu (21.1265S, 174.896E), M 7.3	02/10/2021	22/09, 24/09, 25/09, 01/10
18	Vanuatu (21.1265S, 174.522E), M 6.9	09/10/2021	22/09, 24/09, 25/09, 01/10, 03/10, 04/10
19	Fiji (25.316S, 179.604E), M 6.1	21/10/2021	01/10, 03/10, 04/10, 11/10, 12/10, 18/10, 19/10
20	Labasa, Fiji (16.3139S, 178.578E), M 6.2	19/12/2021	22/11, 28/11, 29/11, 01/12, 04/12, 09/12, 11/12, High solar radiation period (15/12)
21	Levuka, Fiji (18.1104S, 179.352W), M 6.1	26/12/2021	High solar radiation period (15/12, 20/12, 21/12, 22/12, 23/12, 24/12, 25/12)

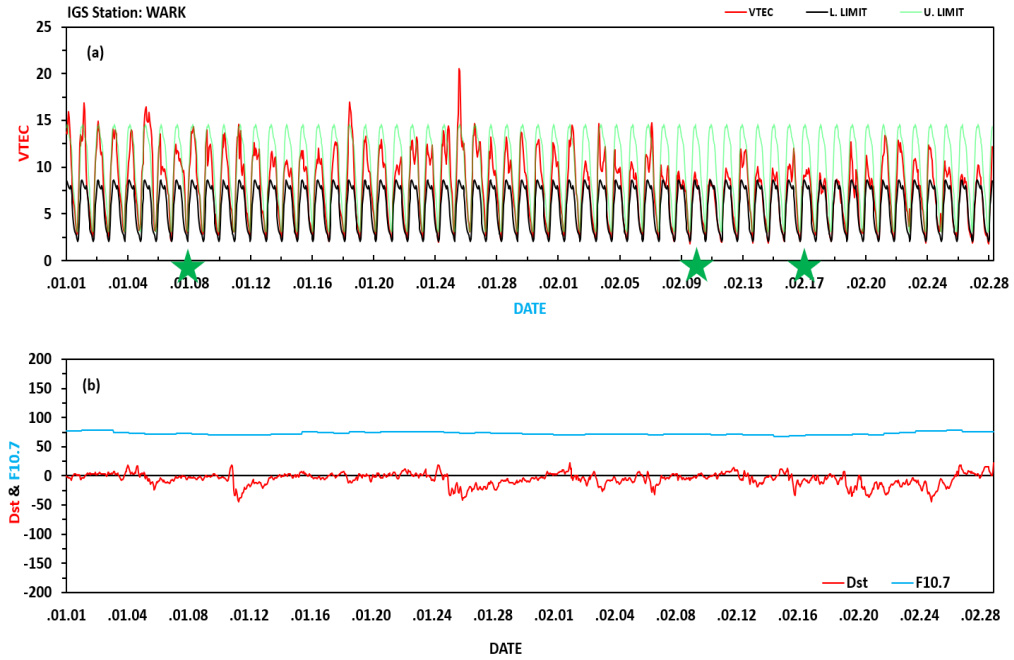

Figure 13 (a) VTEC over the New Zealand region of WARK igs station, from 1st January to 28th February of year 2021. (b) $F_{10.7}$ (Solar flux) and Dst (disturbance in storm time index) data over the same period of time (from 1st January to 28th February). Stars show the day of earthquakes.

Figure 14 (a) VTEC over the New Zealand region of WARK igs station, from 1st March to 30th April of year 2021. (b) $F_{10.7}$ (Solar flux) and Dst (disturbance in storm time index) data over the same period of time (from 1st March to 30th April). Stars show the day of earthquakes.

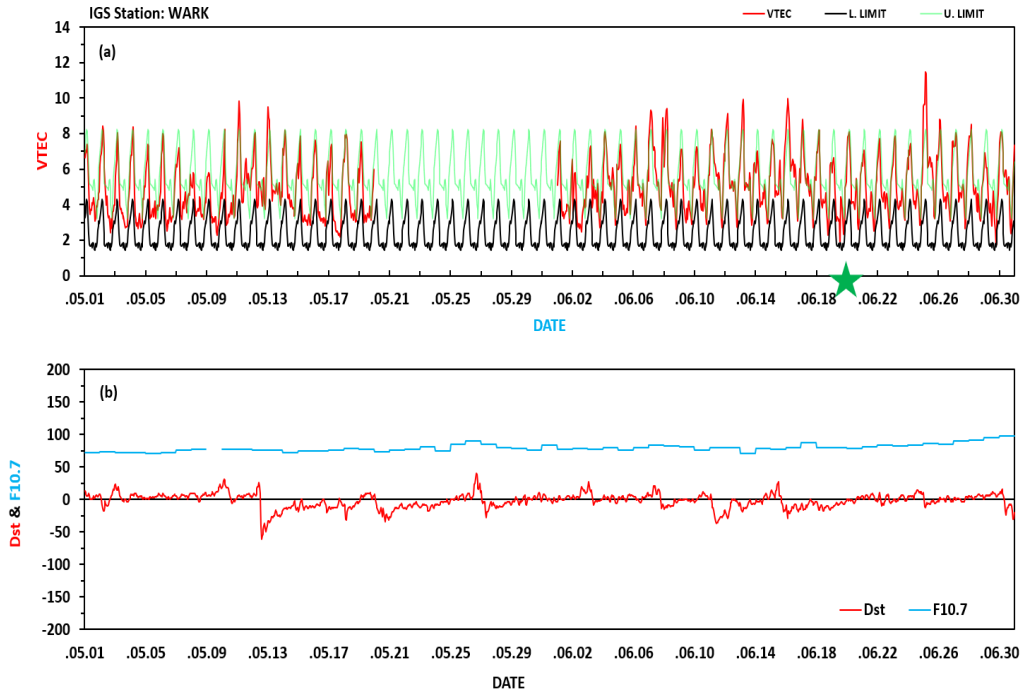

Figure 15 (a) VTEC over the New Zealand region of WARK igs station, from 1st May to 30st June of year 2021. (b) $F_{10.7}$ (Solar flux) and Dst (disturbance in storm time index) data over the same period of time (from 1st May to 30st June). Stars show the day of earthquakes.

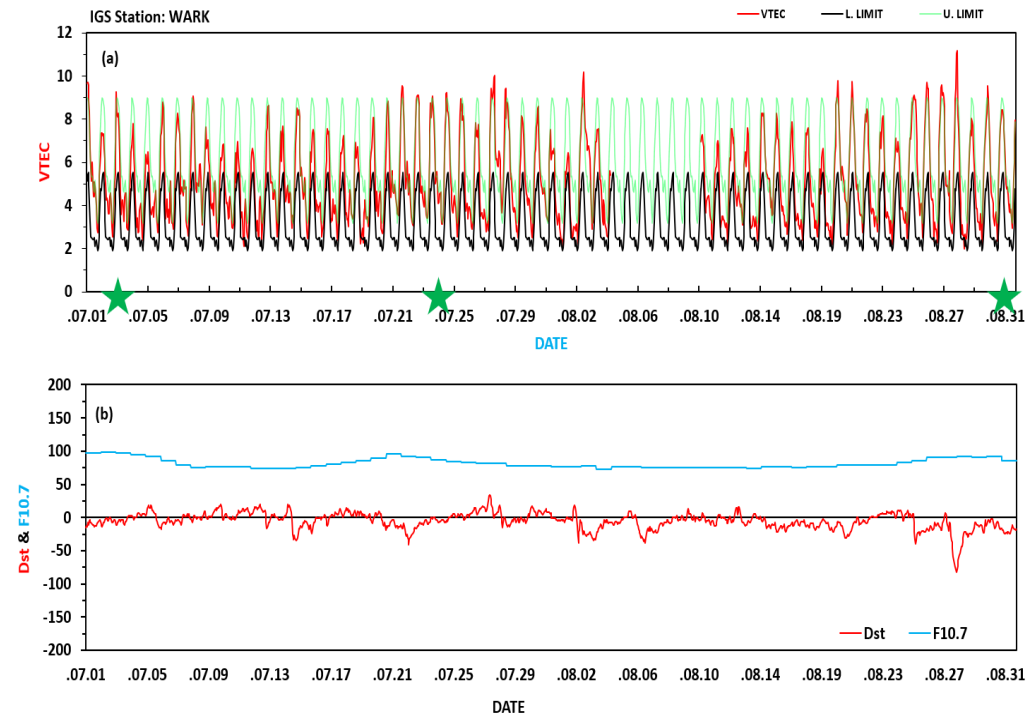

Figure 16 (a) VTEC over the New Zealand region of WARK igs station, from 1st July to 31st August of year 2021. (b) $F_{10.7}$ (Solar flux) and Dst (disturbance in storm time index) data over the same period of time (from 1st July to 31st August). Stars show the day of earthquakes.

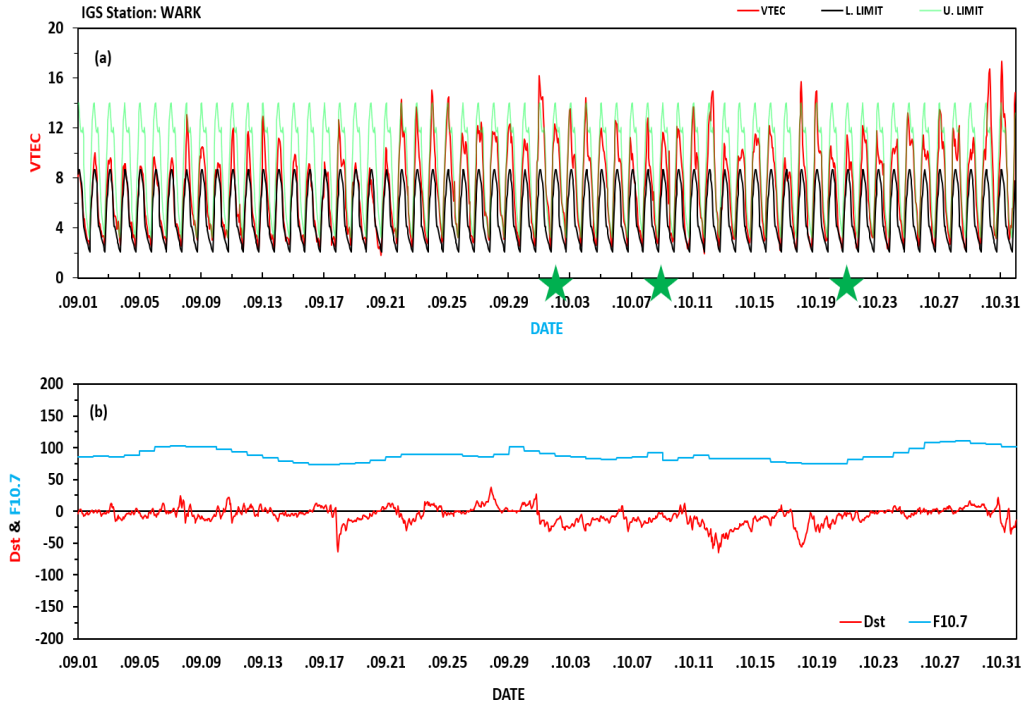

Figure 17 (a) VTEC over the New Zealand region of WARK igs station, from 1st September to 31st October of year 2021. (b) $F_{10.7}$ (Solar flux) and Dst (disturbance in storm time index) data over the same period of time (from 1st September to 31st October). Stars show the day of earthquakes.

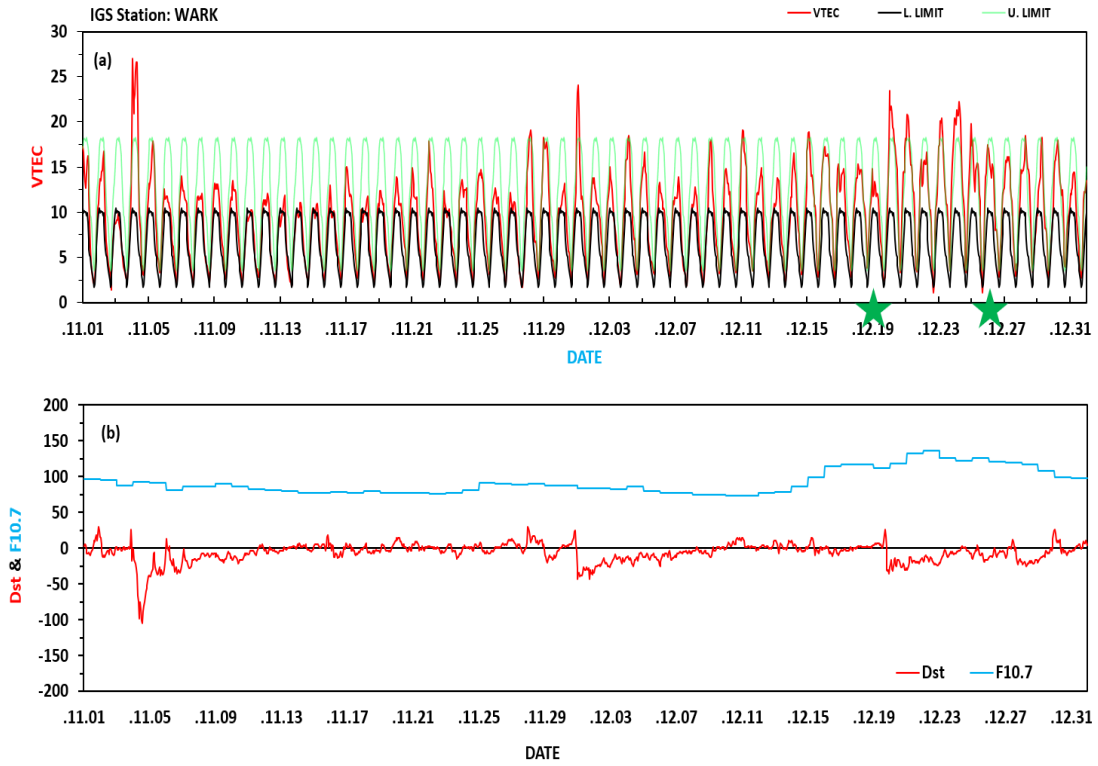

Figure 18 (a) VTEC over the New Zealand region of WARK igs station, from 1st November to 31st December of year 2021. (b) $F_{10.7}$ (Solar flux) and Dst (disturbance in storm time index) data over the same period of time (from 1st November to 31st December). Stars show the day of earthquakes.

Discussion

In the scientific community, there is no consensus on a scientific mechanism to explain recorded ionospheric fluctuation related to earthquakes. Many researchers have seen changes in ionospheric TEC prior to an earthquake [11-24]. According to Parrot [25], the piezoelectric and turbo-electric effects are more likely to be involved in the propagation of the direct wave caused by the compression of rocks near the epicenter. Stress caused by rock appears as an electric charge at the earth's surface and electric current in the atmosphere-ionosphere system [25,27]. The electron concentration in height then is modified or redistributed by an Electric current in the ionosphere and joule heating. It has been observed that rising liquids beneath the earth would release heated gases [28]. Molchanov and Hayakawa [29] suggested that gas water released from the preparatory earthquake zone was the primary source of upward energy fluxes caused by atmospheric gravity waves (AGWs). Natural ionospheric turbulence is modified by the penetration of AGW waves into the ionosphere [30,31]. An electric field parallel to the geomagnetic field line is likely to have resulted from the pre-seismic perpendicular E-field (Electric field) on the earth's surface, which give rise to disruption over the F-region ionosphere. In that zone, perturbing the F-region will cause it to pre-start propagating along conducting M-field (Magnetic-filed) lines and spreading over the larger area [32].

We believe the theory behind the anomaly of TEC given by Pulinets [33], LIAC coupling mechanism;

1) Natural Lithosphere radiation (radon within the locality of active tectonic faults) is the precursory signature of lower and upper atmosphere anomalies discovered 7 - a few days before seismic event near the epicenter.

2) Air ionization created by a-particle radon decay begins the chain of processes involving all layers of atmosphere and region. It results in a great deal of thermal energy release from beneath the surface of crust, and this released heat of transformation allow to run free by water molecules during their attachment to the ions produced by ionization.

3) Heating effects have observed in the sequential chain with some delay from lower to higher atmosphere: Surface latent heat and unusual fluxes of the heat-energy of transformation shown by remote sensing satellites.

4) Variations of tropospheric air phenomenon over the earthquake preparation zone manufacture the local reform of the parameters of electrical Circuit between lithosphere and Ionosphere.

5) Air moves upwards because of latent heat unleash rises further variety of ion clusters nuclei to the altitude of many kilometers resulting in clouds forming. Upwards force field over the seismic active zone.

6) Anomaly generated in atmosphere electricity create impact on the electron density and ion concentration, ion temperature.

7) Contributing electrons modify the D-region of the ionosphere, leading to the abnormal propagation of VLF waves among the waveguide Earth-ionosphere.

8) The planned lay idea delineates the scientific rationale for an integrated observation and validation of earthquake precursors.

Conclusions

We identify abnormal fluctuation in TEC for all 6 earthquakes discussed in this work, consistent with previous publications. Therefore, ionosphere behavior changes a few days before a big seismographic shock inside or distant from the preliminary earthquake zone. Since we are only obtaining dispersed peaks in VTEC, this suggests that the disturbance is caused in TEC by internal factors such as earthquakes rather than solar radiation. Then it is inevitable that not all these deviations are due to volcanic eruptions; instead, that does not happen Day in and Day out. However, this method also has some limitations. TEC is a complex quantity whose variation is affected by solar radiation and seismic activity, so the percentages of TEC of these 2 cannot be separated. It clearly shows that day-to-day maximum VTEC before and after the earthquake is in a specific latitude range from the earthquake's epicenter. As a result, we can say if these variations in tec are close to the epicenter.

Acknowledgements

I would like to take this opportunity and pleasure to recognize the contributions of many individuals who have been inspirational and supportive throughout my work and have endowed me with the most valuable knowledge to my endeavor succeeds. All of those individuals left their mark on my work, and I will always be grateful to them. I appreciate the facilities provided to me for my work by Dr. S. S. Pancholi, Executive Dean of the Faculty of Sciences at Ganpat University, and Dr. Amit K. Parikh, Dean of the

Faculty of Sciences at Ganpat University and Principal of the Mehsana Urban Institute of Sciences who offered me helpful assistance.

References

[1] B Isacks, J Oliver and LR Sykes. Seismology and the new global tectonics. *J. Geophys. Res.* 1968; **73**, 5855-99.

[2] AA Tronin. *Satellite thermal survey application for earthquake prediction*. *In*: M Hayakawa (Ed.). Atmospheric and Ionospheric Electromagnetic Phenomena Associated with Earthquakes, Terrapub, Tokyo, Japan, 1999, p. 717-46.

[3] VA Liperovsky CV Meister, VV Mikhailin, VV Bogdanov, PM Umarkhodgaev and EV Liperovskaya. Electric field and infrared radiation in the troposphere before earthquakes. *Nat. Hazards Earth Syst. Sci.* 2011; **11**, 3125-33.

[4] SA Pulinets, D Ouzounov, A Karelin, KA Boyarchuk and LA Pokhmelnykh. The physical nature of thermal anomalies observed before strong earthquakes. *Phys. Chem. Earth A B C* 2006; **31**, 143-53.

[5] MA Freeshah, X Zhang, J Chen, Z Zhao, N Osama, M Sadek and N Twumasi. Detecting ionospheric TEC disturbances by three methods of detrending through dense CORS during a strong thunderstorm. *Ann. Geophys.* 2020; **63**, GD667.

[6] I Toman, D Brčić and S Kos. Contribution to the research of the effects of etna volcano activity on the features of the ionospheric total electron content behaviour. *Rem. Sens.* 2021; **13**, 1006.

[7] V Singh, V Chauhan, OP Singh and B Singh. Ionospheric effect of earthquakes as determined from ground based TEC measurement and satellite data. *Indian J. Radio Space Phys.* 2010; **39**, 63-70.

[8] KS Yadav, SP Karia and KN Pathak. Removal of solar radiation effect based on nonlinear data processing technique for seismo-ionospheric anomaly before few earthquakes. *Geomatics Nat. Hazards Risk* 2016; **7**, 1147-61.

[9] PVR Rao, K Niranjan, DS Prasad, SG Krishna and G Uma. On the validity of the ionospheric pierce point (IPP) altitude of 350 km in the Indian equatorial and low-latitude sector. *Ann. Geophys.* 2006; **24**, 2159-68.

[10] SC Chakravarty. A novel approach to study regional ionospheric variations using a real-time TEC model. *Positioning* 2014; **5**, 1-11.

[11] M Devi, AK Barbara and A Depueva. Association of total electron content (TEC) and foF2 variations with earthquake events at the anomaly crest region. *Ann. Geophys.* 2004; **47**, 83-91.

[12] SP Karia and KN Pathak. Change in refractivity of the atmosphere and large variation in TEC associated with some earthquakes, observed from GPS receiver. *Adv. Space Res.* 2011; **47**, 867-76.

[13] M Akhoondzadeh and MR Saradjian. TEC variations analysis concerning Haiti (January 12, 2010) and Samoa (September 29, 2009) earthquakes. *Adv. Space Res.* 2011; **47**, 94-104.

[14] K Yadav, SP Karia and KN Pathak. Anomalous variation in GPS TEC, land and ocean parameters prior to 3 earthquakes. *Acta Geophys.* 2016; **64**, 43-60.

[15] KS Yadav and JS Pathak. Anomalous variation in GPS based total electron content (TEC), prior to six (6) earthquakes in 2016. *Mausam* 2018; **69**, 419-26.

[16] M Ulukavak, M Yalçınkaya, ET Kayıkçı, S Öztürk, R Kandemir and H Karsli. Analysis of ionospheric TEC anomalies for global earthquakes during 2000 - 2019 with respect to earthquake magnitude (MW ≥ 6.0). *J. Geodyn.* 2020; **135**, 101721.

[17] M Ulukavak and M Yalcinkaya. Precursor analysis of ionospheric GPS-TEC variations before the 2010 M 7.2 Baja California earthquake. *Geomatics Nat. Hazards Risk* 2017; **8**, 295-308.

[18] G Sharma, PKC Ray, S Mohanty and S Kannaujiya. Ionospheric TEC modelling for earthquakes precursors from GNSS data. *Quaternary Int.* 2017; **462**, 65-74.

[19] D Pundhir, B Singh and OP Singh. Anomalous TEC variations associated with the strong Pakistan-Iran border region earthquake of 16 April 2013 at a low latitude station Agra, India. *Adv. Space Res.* 2014; **53**, 226-32.

[20] M Akhoondzadeh. Anomalous TEC variations associated with the powerful Tohoku earthquake of 11 March 2011. *Nat. Hazards Earth Syst. Sci.* 2012; **12**, 1453-62.

[21] MA Tariq, M Shah, M Hernández-Pajares and T Iqbal. Pre-earthquake ionospheric anomalies before three major earthquakes by GPS-TEC and GIM-TEC data during 2015-2017. *Adv. Space Res.* 2019; **63**, 2088-99.

[22] J Guo, W Li, X Liu, J Wang, X Chang and C Zhao. On TEC anomalies as precursor before MW 8.6 Sumatra earthquake and MW 6.7 Mexico earthquake on April 11, 2012. *Geosci. J.* 2015; **19**, 721-30.

[23] S Asaly, LA Gottlieb, N Inbar and Y Reuveni. Using support vector machine (SVM) with GPS ionospheric TEC estimations to potentially predict earthquake events. *Rem. Sens.* 2022; **14**, 2822.
[24] P Xiong, C Long, H Zhou, X Zhang and X Shen. GNSS TEC-based earthquake ionospheric perturbation detection using a novel deep learning framework. *IEEE J. Sel. Top. Appl. Earth Observations Rem. Sens.* 2022; **15**, 4248-63.
[25] M Parrot. Use of satellites to detect seismo-electromagnetic effects. *Adv. Space Res.* 1995; **15**, 27-35.
[26] FT Freund. Pre-earthquake signals-part II: Flow of battery currents in the crust. *Nat. Hazards Earth Syst. Sci.* 2007; **7**, 543-8.
[27] S Uyeda, T Nagao and M Kamogawa. Short-term earthquake prediction: Current status of seismo-electromagnetics. *Tectonophysics* 2009; **470**, 205-13.
[28] VN Troyan and M Hayakawa, M. (2002). *Seismo electromagnetics: Lithosphere-atmosphere-ionosphere coupling*. Terra Scientific Publishing Company, Finland, 2002, p. 215-21.
[29] OA Molchanov and M Hayakawa. *Seismo-electromagnetics and related phenomena: History and latest results.* Terrapub, Tokyo, Japan, 2008.
[30] VA Liperovsky, OA Pokhotelov, EV Liperovskaya, MM Parrot, CV Meister and OA Alimov. Modification of sporadic E-layers caused by seismic activity. *Surv. Geophys.* 2000; **21**, 449-86.
[31] O Molchanov, E Fedorov, A Schekotov, E Gordeev, V Chebrov, V Surkov. Lithosphere-atmosphere-ionosphere coupling as governing mechanism for preseismic short-term events in atmosphere and ionosphere. *Nat. Hazards Earth Syst. Sci.* 2004; **4**, 757-67.
[32] JAY Liu, YI Chen, YJ Chuo and CS Chen. A statistical investigation of pre-earthquake ionospheric anomaly. *J. Geophys. Res.* 2006; **111**, A05304.
[33] SOD Pulinets. Lithosphere-atmosphere-ionosphere coupling (LAIC) model: An unified concept for earthquake precursors validation. *J. Asian Earth Sci.* 2011; **41**, 371-82.